

Jingyuan Xu
Virgile Viasnoff
Denis Wirtz

Compliance of actin filament networks measured by particle-tracking microrheology and diffusing wave spectroscopy

Received: 3 April 1998
Accepted: 26 May 1998

Abstract We monitor the time-dependent shear compliance of a solution of semi-flexible polymers, using diffusing wave spectroscopy (DWS) and video-enhanced single-particle-tracking (SPT) microrheology. These two techniques use the small thermally excited motion of probing microspheres to interrogate the local properties of polymer solutions. The solutions consist of networks of actin filaments which are long semi-flexible polymers. We establish a relationship between the mean square displacement (MSD) of microspheres imbedded in the solution and the time-dependent creep compliance of the solution, $\langle \Delta r^2(t) \rangle = (k_B T / \pi a) J(t)$. Here, $J(t)$ is the creep compliance, $\langle \Delta r^2(t) \rangle$ is the mean-square displacement, and a is the radius of the microsphere chosen to be larger than the mesh size of the polymer network. DWS allows us to measure mean square displacements with microsecond temporal resolution and Ångström spatial resolution. At short times, the mean square displacement of a 0.96 μm diameter sphere in a concentrated actin solution displays sub-diffusion. $\langle \Delta r^2(t) \rangle \propto t^\alpha$, with a characteristic exponent

$\alpha = 0.78 \pm 0.05$, which reflects the finite rigidity of actin. At long times, the MSD reaches a plateau, with a magnitude that decreases with concentration. The creep compliance is shown to be a weak function of polymer concentration and scales as $J_p \propto c^{-1.2 \pm 0.3}$. This exponent is correctly described by a recent model describing the viscoelasticity of semi-flexible polymer solutions. The DWS and video-enhanced SPT measurements of the compliance plateau agree quantitatively with compliance measured independently using classical mechanical rheometry for a viscous oil and for a solution of flexible polymers. This paper extends the use of DWS and single-particle-tracking to probe the local mechanical properties of polymer networks, shows for the first time the proportionality between mean square displacement and local creep compliance, and therefore presents a new, direct way to extract the viscoelastic properties of polymer systems and complex fluids.

Key words Actin – rheology – diffusing wave spectroscopy

J. Xu · V. Viasnoff
Department of Chemical Engineering
The John Hopkins University
3400 North Charles Street
Baltimore, MD 21218
USA

D. Wirtz (✉)
Chemical Engineering
G. W. C. Whiting School of Engineering
The John Hopkins University
3400 North Charles Street
Baltimore, MD 21218-2694
USA
e-mail: wirtz@jhu.edu

Introduction

The rheology of semi-flexible polymers is more complex than that of flexible and rigid polymers (de Gennes, 1979; Doi and Edwards, 1989; Ferry, 1980). The description of semi-dilute and concentrated solutions of semi-flexible polymers is greatly complicated by the presence of an additional intermediate length scale, outside the monomer size and the polymer contour length: the persistence length. If the persistence length, which describes the finite rigidity of a polymer, is of the order of magnitude of the contour length L and much larger than the diameter, the polymer is semi-flexible (Doi and Edwards, 1989).

Filamentous actin (F-actin), the polymerized form of the globular four-lobed protein actin (G-actin), forms long semi-flexible polymers with a diameter $d=7$ nm (Alberts et al., 1994). The persistence length of F-actin, l_p , has been measured using different techniques, including dynamic light scattering, video-microscopy, and electron microscopy (Gittes et al., 1993; Isambert et al., 1995; Muller et al., 1991). Most of these approaches have confirmed that F-actin is a semi-flexible polymer, i.e. $d \ll l_p \leq L$. Furthermore, the rigidity and contour length of F-actin can be finely controlled by regulating proteins, such as α -actinin (crosslinking proteins), gelsolin (capping and severing proteins), and actophorin (severing proteins) (Alberts et al., 1994; Isambert et al., 1995). The relatively good control of the intrinsic properties of F-actin makes it an ideal polymer to investigate the linear viscoelasticity of concentrated solutions of semi-flexible polymers.

Due to its importance in providing non-muscle cells with structural rigidity, the rheology of actin has been studied extensively (Alberts et al., 1994). However, until recently, these rheological studies have primarily focused on the magnitude of the plateau modulus that actin solutions display at small frequencies (Haskell et al., 1994; Janmey et al., 1988, 1990, 1994; Sato et al., 1987; Tempel et al., 1996; Wachsstock et al., 1993; Wachsstock et al., 1994; Xu et al., 1998c; Zaner and Hartwig, 1988). The magnitude of this plateau modulus and, therefore, the nature of the viscoelastic properties of actin solutions, has, however been the subject of much debate. This debate has been recently resolved by Xu et al. (1998a), who unambiguously showed that careless preparation and storage of actin can dramatically increase the small-frequency elastic modulus of the solution. We also recently showed how small amounts of crosslinking proteins can greatly increase the elastic modulus, especially at large strains (Palmer et al., 1998). Both papers showed the absolute necessity of using fresh, non-frozen actin, uncontaminated by crosslinking proteins. In this paper, we use recent advances in actin preparation, which eliminate crosslinking and capping proteins.

In order to probe the dynamics of actin motion in concentrated solutions, we use two complementary approaches: mechanical rheometry and particle-tracking microrheology. Particle-tracking microrheology, which involves either diffusing wave spectroscopy (Mason et al., 1997b; Mason and Weitz, 1995; Palmer et al., 1998) or single particle-tracking microrheology (Gittes et al., 1997; Mason et al., 1997a,b; Schnurr et al., 1997), is based on the high-resolution measurement of the mean square displacement (MSD) of microspheres imbedded in the polymer solution to be probed. DWS, as developed by Mason and Pine (Mason and Weitz, 1995) spectroscopically monitors the thermally excited motion of many spheres mixed with the polymer solution; particle-tracking microrheology as developed by Kuo, Wirtz, and coworkers (Mason et al., 1997a,b; Palmer et al., 1998) monitors the two-dimensional motion of a *single* microsphere in the *temporal* domain. Thus far, different analytical schemes have been used to extract the elastic and loss moduli of the solution (Mason et al., 1997b; Mason and Weitz, 1995; Schnurr et al., 1997). These schemes involve multiple transformation steps of the real space measurements of the MSD or the spectrum of the MSD, to the Laplace space calculation of a viscoelastic modulus, to the use of Kramers-Kronig relations, and finally via complex transformation to the elastic and loss moduli. Typically, these multiple-step schemes, while powerful in generating linear viscoelastic moduli, truncate several temporal decades at small and large time scales. This paper proposes a much more direct interpretation of MSD measurements: we show that the measured MSD is simply proportional to the time-dependent shear creep compliance, which contains a great deal of the interesting rheological information.

In order to demonstrate the effectiveness of our approach, we independently measure the creep compliance $J(t)$ of actin solutions using particle-tracking microrheometry and mechanical rheometry. We observe excellent agreement between these independent measurements. As a further control, we measure the creep compliance of a viscous oil and of a semi-dilute solution of flexible polymers, polyethylene oxide in water, and obtain excellent agreement.

Particle-tracking measurements by DWS offer a much extended temporal range especially at short time scales, smaller than 10^{-5} s, which cannot be probed by mechanical rheometry in one measurement. At these short times, we find that $J(t)$ increases with an effective power law of time, $J(t) \propto t^\alpha$ with $\alpha=0.78 \pm 0.05$, in agreement with a recent model by Morse (Morse, 1997), which predicts $\alpha=3/4$. This exponent reflects the finite rigidity of F-actin and the resulting liquid-like behavior of the F-actin networks at short times. We also find that the short-time compliance scales with the inverse of the square root of actin concentration, $J \propto c^{-0.50}$ for $t < 10^{-3}$ s. At times between 10^{-1} and 10^4 s as

probed by video-enhanced SPT and mechanical rheometry, $J(t)$ reaches a “plateau” J_p , which corresponds to a slowed increase of the creep at long times. For those intermediate time scales, the creep has a concentration-dependent magnitude which scales as $J_p \propto c^{-\beta}$ with $\beta = 1.3 \pm 0.2$. Here again, this exponent is in qualitative agreement with Morse’s model (Morse, 1997), which describes the long-time scale viscoelasticity of solutions of semi-flexible polymers. Morse’s model is based on the reptation model of de Gennes (de Gennes, 1979) and Doi and Edwards (Doi and Edwards, 1989), which assumes that the shear stress relaxes when polymers can escape the tube inside which each polymer is confined by surrounding polymers. Morse’s model predicts $\beta = 1.4$, as opposed to $\beta = 2.2$ for solutions of flexible polymers, and assumes that the elasticity of a semi-flexible polymer network results from the forces preventing transverse distortion of the polymer tube conformation (Morse, 1997).

Experimental techniques

Actin preparation

Actin is extracted from rabbit skeletal muscle acetone powder by the method of Spudich and Watt (Spudich and Watt, 1971). The resulting actin is gel filtered on Sephacryl S-300 HR instead of Sephadex G-150 (MacLean-Fletcher and Pollard, 1980). The purified actin is stored as Ca^{2+} -actin in continuous dialysis at 4°C against daily changed buffer G (0.2 mM ATP, 0.5 mM DTT, 0.1 mM CaCl_2 , 1 mM NaAzide, and 2 mM Tris-Cl, pH 8.0). The final actin concentration is determined by ultra-violet absorbance at 290 nm, using an extinction coefficient of $2.66 \times 10^4 \text{ M}^{-1} \text{ cm}^{-1}$, and a cell path length of 1 cm. Ca^{2+} and Mg^{2+} actin filaments are generated by adding 0.1 volume of $10 \times \text{KMC}$ (500 mM KCl, 10 mM MgCl_2 , 1 mM CaCl_2 , 20 mM Tris-Cl, pH 8) and 10-x KME (500 mM KCl, 10 mM MgCl_2 , 10 mM EGTA, 100 mM imidazole, pH 7.0) polymerizing salt buffer solution to 0.9 volume of G-actin in buffer G, respectively. The actin used for all experiments comes from the last fraction of the actin peak obtained by one gel filtration.

Diffusing wave spectroscopy (DWS) and video-enhanced single-particle-tracking rheology (SPT)

The beam from an Ar^+ -ion laser operating in the single-line-frequency mode at a wavelength of 514 nm is focused and incident upon a flat scattering cell which contains the polymerized actin solution and spherical

optical probes. The light multiply-scattered from the solution is collected by two photomultiplier tubes (PMT) via a single-mode optical fiber with a collimator lens of very narrow angle of acceptance at its front end and a beamsplitter at its back end. The outputs of the PMTs are directed to a correlator working in the pseudo cross-correlation mode to generate the autocorrelation function $g_2(t) - 1$ from which quiescent rheological properties of the actin solutions can be calculated (Palmer et al., 1998).

Actin is polymerized in situ for 12–14 h before measurement by loading the scattering cell with a solution of monomeric actin mixed with the polymerizing salt solution and a dilute suspension of monodisperse latex microspheres (Duke Scientific Corp.) of diameter 0.96 μm at a volume fraction of 0.01. The scattering cell is then immediately capped tightly. We verified by both time-resolved static light scattering and time-resolved mechanical rheology that G-actin was fully polymerized into F-actin at all concentrations presented in this paper before 12 h. Using static light scattering, we verified that more than 95% of the scattering intensity in the transmission geometry was due to the microspheres, less than 5% due to the actin filament network itself. We also verified using mechanical rheology that the added latex beads did not affect the rheology of polymerized actin, representing less than 5–7% of the magnitude of $G'(\omega)$ and $G''(\omega)$ at all actin concentrations used in this paper. All DWS measurements are conducted at a temperature of $T = 23^\circ\text{C}$.

In addition to DWS, we conduct video-enhanced single-particle-tracking (SPT) microrheology measurements. Briefly (Mason et al., 1997a), an extremely dilute suspension of 0.96 μm diameter microspheres is mixed with an unpolymerized G-actin solution. Polymerizing salt is added, which promotes the self-assembly of G-actin into long semi-flexible F-actin polymers. After approximately 10 h of curing, an elastic F-actin network forms. The position of a single bead is tracked with 5–10 nm resolution by monitoring the center-of-mass displacements of the two-dimensional light intensity of the Airy figure of the microsphere. The rate of data acquisition for video-enhanced SPT is slightly smaller than the video rate of image acquisition. Therefore, the maximum frequency of viscoelastic moduli which can be probed by that technique is about 5 Hz. For each system, we monitor between 15 and 30 microspheres, we conduct five independent measurements on each bead, and on three different samples of actin at each actin concentration. Further details about our video-microscopy based, single particle-tracking microrheometer (SPT) are given in Mason et al. 1997a).

Advantages of particle-tracking microrheometry (DWS and video-enhanced SPT) include the possibly to generate viscoelastic moduli without subjecting the specimen to shear, which can induce bundling of the

polymers. Video-enhanced SPT also allows to extract viscoelastic moduli that are anisotropic and require extremely small sample volumes $\approx 20 \mu\text{l}$, as opposed to $\approx 1 \text{ ml}$ for a regular rheometer and for the DWS instrument. Furthermore, video-enhanced SPT is relatively simple to implement. Note, however, that DWS generates viscoelastic moduli over an extremely large range of frequencies, 2 to 5 decades wider than probed by classical rheometry and video-enhanced SPT.

Mechanical rheometry

In order to compare our optical measurements with classical mechanical measurements, we employ a stress-controlled mechanical rheometer (Rheometrics and Haake) equipped with a 40 or 50 mm diameter cone and plate geometry and a strain-controlled rheometer (Rheometrics) with rapid control of the stress. To prevent possible evaporation effects, the cone and plate tools are enclosed in a custom-made vapor trap and sealed at the edges with an hydrophobic oil. The temperature of the sample is fixed at $T=23^\circ\text{C}$ to within 0.1°C . The G-actin solution is placed between the cone and plate tools and allowed to polymerize in the presence of polymerizing salt for 12–14 h, prior to the measurements. The linear and nonlinear viscoelastic properties of actin solutions, PEO solutions, are also found to be unaffected by the presence of the probing microspheres.

Theory

Derivation and interpretation of the relation between mean-square displacement and creep compliance

In this section, we establish a relationship between the mean square displacement of a microsphere imbedded in a viscoelastic fluid and the shear creep compliance of that fluid. The local viscoelastic modulus of a fluid and the mean square displacement of a microsphere suspended in that fluid can be related *via* (Mason and Weitz, 1995)

$$\tilde{G}(s) = \frac{s}{6\pi a} \left[\frac{6k_B T}{s^2 \langle \Delta \tilde{r}^2(s) \rangle} - ms \right] \approx \frac{k_B T}{\pi a s \langle \Delta \tilde{r}^2(s) \rangle}, \quad (1)$$

Here, k_B is Boltzmann's constant, T is the temperature of the sample, a is the radius of the microsphere, m is its mass, s is the Laplace frequency, and $\tilde{\cdot}$ represents the unilateral Laplace transformation defined as $\tilde{X}(s) \equiv L[X(t)] \equiv \int_0^\infty X(t) \exp(-st) dt$. Equation (1) relates the unilateral Laplace transform of the stress re-

laxation modulus $G_r(t)$, $\tilde{G}(s) \equiv s\tilde{G}_r(s)$, to the Laplace transform of the mean-square displacement $\langle \Delta r^2(t) \rangle$. While Eq. (1) is model-dependent, it is interesting to note that it yields the correct results for the extreme cases of a purely viscous liquid and a purely elastic solid. For a viscous liquid, $\langle \Delta \tilde{r}^2(s) \rangle = 6D/s^2 = k_B T / \pi \eta a s^2$ and $\tilde{G}(s) = \eta s$, where η is the constant viscosity of the liquid; therefore $G'(\omega) = 0$ and $G''(\omega) = \eta_s \omega$. Instead, for an elastic solid, $\langle \Delta \tilde{r}^2(s) \rangle = r_0^2$ and $\tilde{G}(s) = G_0 = k_B T / \pi a r_0^2$, where G_0 is the elastic modulus; therefore, $G'(\omega) = G_0$ and $G''(\omega) = 0$.

Now, we relate the creep compliance to the viscoelastic modulus. The shear stress and shear strain are related to one another as

$$\tau(t) = - \int_0^t G_r(t-t') \dot{\gamma}(t') dt' \quad (2)$$

$$\gamma(t) = \int_0^t J(t-t') \dot{\tau}(t') dt' \quad (3)$$

where $\dot{\tau} = d\tau/dt$ and $\dot{\gamma} = d\gamma/dt$ are the rates of change of the shear stress and shear strain, $G_r(t)$ is the linear stress relaxation modulus, and $J(t)$ is the linear creep compliance. Physically, $G_r(t)$ is the stress generated by a step strain $\gamma = \gamma_0 H(t)$, where $H(t)$ is a Heaviside function and $J(t)$ is the strain resulting from a step of stress $\tau = \tau_0 H(t)$. For instance, for an elastic solid

$$G_r(t) = G_0 \quad \text{and} \quad J(t) = \frac{1}{G_0} \quad (4)$$

For a purely viscous fluid of viscosity η ,

$$G_r(t) = \eta \delta(t) \quad \text{and} \quad J(t) = \frac{t}{\eta} H(t) \quad (5)$$

Unilateral Laplace transformation of Eqs. (2) and (3) yields simple relationships between the transforms $\tilde{J}(s)$, $\tilde{G}(s)$, and $\tilde{\gamma}(s)$:

$$\tilde{\tau}(s) = s\tilde{G}_r(s)\tilde{\gamma}(s) = \tilde{G}(s)\tilde{\gamma}(s) \quad (6)$$

$$\tilde{\gamma}(s) = s\tilde{J}(s)\tilde{\tau}(s). \quad (7)$$

Hence,

$$s\tilde{J}(s)\tilde{G}(s) = 1, \quad (8)$$

which establishes a relation between the Laplace transforms of the creep compliance and of the stress relaxation modulus. Since $s\tilde{G}(s)\langle \Delta \tilde{r}^2(s) \rangle = k_B T / \pi a$ (see Eq. (1)), we can directly relate $\langle \Delta \tilde{r}^2(s) \rangle$ to $\tilde{J}(s)$ as

$$\langle \Delta \tilde{r}^2(s) \rangle = \frac{k_B T}{\pi a} \tilde{J}(s)$$

or

$$\langle \Delta r^2(t) \rangle = \frac{k_B T}{\pi a} J(t) \quad (9)$$

using $J(0) = 0$ for a viscoelastic fluid. This last equation is the central relationship of this paper, which we test experimentally by measuring independently $\langle \Delta r^2(t) \rangle$ and $J(t)$ by particle-tracking and by mechanical rheometry, respectively. Equation (9) neglects inertial effects, which become important at times scales $t < 10^{-6}$ s. But here again, Eq. (9) yields the correct results for the extreme cases of a purely viscous fluid and a purely elastic solid. For a viscous liquid, $\langle \Delta r^2(t) \rangle = 6DtH(t) = (k_B T \pi \eta a) t H(t)$ and $J(t) = (t/\eta)H(t)$, which verifies Eq. (5). For an elastic solid, $\langle \Delta r^2(s) \rangle = r_0^2$ and $J(t) = 1/G_0$, where $G_0 = k_B T / \pi a r_0^2$, which verifies Eq. (4).

This simple relation between mean-square displacement and the creep compliance can be further interpreted as follows. A microsphere of radius a imbedded in a complex fluid is subject to an average thermal Brownian force of amplitude $k_B T/a$. The resulting stress on the surrounding fluid is proportional to $k_B T/a^3$. The strain is therefore proportional to the creep. Since the strain is the divergence of the displacement, it is proportional to $\langle \Delta r^2(t) \rangle / a^2$. Therefore, $\langle \Delta r^2(t) \rangle / a^2 \propto J(t) k_B T / a^3$.

Equation (8) can also be projected into the temporal domain:

$$J(0)G_r(t) + \int_0^t \frac{dJ}{dt'}(t-t')G_r(t')dt' = H(t) \quad (10)$$

Using $J(0) = 0$, this last relation can be rewritten as a Volterra equation

$$\int_0^t J(t-t')G_r(t')dt' = tH(t) \quad (11)$$

Since $J(t)$ is proportional to $\langle \Delta r^2(t) \rangle$, one could use this last integral relation to numerically extract the stress relaxation modulus from optically measured mean square displacements.

Results and discussion

We present measurements of the shear compliance of actin filament networks obtained by single particle-tracking (SPT), diffusing wave spectroscopy (DWS), and mechanical rheometry. These measurements achieve three objectives: to gain a new insight into the fast dynamics of motion of individual filaments at short times, which is dominated by bending fluctuations, to further test Morse's model of rheology of concentrated solutions of semi-flexible polymers, and to establish a fun-

damental relationship between mean square displacement as measured by DWS and SPT and compliance as measured by mechanical rheometry.

DWS and video-enhanced SPT measurements of mean-square displacement

The mean-square displacement of a microsphere imbedded in a polymer solution can be measured in two ways. The mean square displacement is either measured directly from the two-dimensional trajectories of a single microsphere or indirectly from the autocorrelation function of the light multiply scattered by an ensemble of microspheres. The former approach involves the use of a two-dimensional single-particle-tracking technique (Mason et al., 1997b; Palmer et al., 1998). The latter approach involves the use of diffusing wave spectroscopy (Mason et al., 1997b; Mason and Weitz, 1995; Palmer et al., 1998). This paper presents mean square displacement measurements using the two techniques. However, DWS has a bandwidth superior to video-enhanced particle-tracking. Here, we present video-enhanced particle-tracking measurements to demonstrate that a cheaper microscope can provide for a relatively quantitative measurement of the creep at small frequencies. For both techniques, we use 0.96 μm diameter microspheres, which are mixed with the G-actin solution at small volume fractions. Salt, which promotes G-actin self-assembly, is added to the mixture and mean square displacements are collected after 12–14 h, the time it takes for the elasticity of the F-actin network to reach a steady state, as verified by mechanical rheometry.

Selection of a probing microsphere follows strict criteria. The microsphere cannot be smaller than the mesh size of the actin network because the relationship between the local displacements of a microsphere in a fluid as described by Eq. (1) and the macroscopic viscoelasticity of that fluid is valid as long as the size of the bead is much larger than the mesh size of the network. This is because the Langevin equation describing the thermally-excited motion of the bead and underlying Eq. (1) is valid in the continuous limit for which the network-generating viscoelasticity forms a continuum for the motion of the bead. Also, the hydrodynamic interactions which scales as r^{-1} ought to encompass a sufficiently large number of entanglements, which is the case when the network is tight or when the bead is large. The bead cannot be too large, however. If the bead is much larger than the mesh, it sediments, its motion is anisotropic and is governed by the macroscopic viscosity of the suspending fluid. Also, the bead cannot bind chemically to the polymer network because its long-time, large-length-scale displacements would be artificially hindered, which could generate spurious results in the calculation of the creep compliance and the

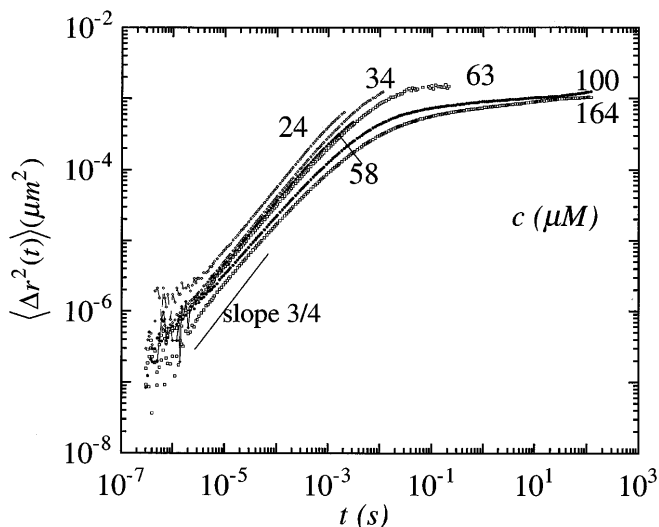


Fig. 1 Mean square displacements of 0.965 μm diameter latex microspheres imbedded in F-actin solutions of increasing concentrations as measured by diffusing wave spectroscopy. Even at the shortest time scales, the motion of the microspheres is sub-diffusive, $\langle \Delta r^2(t) \rangle \propto t^\alpha$ with $\alpha < 1$ because the microspheres' motion is elastically hindered by the dense actin network, which has a mesh size smaller than the bead size. The exponent α is $\alpha = 0.78 \pm 0.05$, and is independent of actin concentration

viscoelastic moduli. Using analytical centrifugation and gel electrophoresis, we checked that latex beads and actin do not bind to one another. Finally, in the case of DWS, the concentration of microspheres should be large enough to allow for the limit of multiple scattering to be reached, but not too large since hydrodynamic interactions between probing microspheres can cause biased motion, which is not taken into account in Eq. (1).

Figure 1 displays the mean square displacement of 0.96 μm diameter microspheres measured by diffusing wave spectroscopy. Over the limited range of time scales probed by video-enhanced SPT, we observe a fair agreement between the two particle-tracking measurements. We measure mean square displacements over an extended range of actin concentrations. For all actin concentrations tested, the mean square displacement undergoes a sequence of dynamical transitions which are directly related to the short-time and long-time dynamics of the actin filaments surrounding the probing microsphere. At short times and over more than two temporal decades, until a crossover time τ_e the mean square displacement grows with a characteristic power law of time:

$$\langle \Delta r^2(t) \rangle \propto t^\alpha \quad \alpha = 0.78 \pm 0.10 \quad \text{for } t < \tau_e \quad (13)$$

This last result implies that the motion of a microsphere in a tight F-actin network is subdiffusive ($\alpha < 1$) even at the shortest probed time scales, i.e. down to 10^{-6} s.

The exponent α reflects the finite, local rigidity of actin filaments. A recent model by Morse (1997) predicts that the viscoelastic modulus of a solution of semi-flexible polymer displays a power law behavior at high-frequencies as $|G^*(\omega)| \propto \omega^{3/4}$ which, according to Eq. (1), predicts $\alpha = 3/4$, in excellent agreement with our high resolution MSD. Also, an exponent $\alpha = 1/2$ is predicted by the Rouse model in the case of a flexible-polymer network for which hydrodynamic interactions are ignored (Doi and Edwards, 1989), which further confirms our interpretation of α . This exponent can also be interpreted as the phase shift between loss and storage moduli at high frequencies. In the power law regime at large frequencies or small time scales, if $G^*(\omega) \propto (i\omega)^\alpha$, then $G''/G' = \tan(\pi\alpha/2)$. For instance, if the fluid surrounding the microsphere is purely viscous, $G' = 0$ and $\alpha = 1$, if the fluid is purely elastic, $G'' = 0$ and $\alpha = 0$. Therefore, α also reflects the viscoelastic nature of the fluid at high frequencies, determining if dissipation or elasticity dominates at short time scales. Since the power law behavior $\langle \Delta r^2(t) \rangle \propto t^{3/4}$ extends over more than two decades, the viscoelastic modulus has a power law behavior over an extended frequency range as $G^*(\omega) \propto (i\omega)^{3/4}$. As a result, the loss modulus dominates the storage modulus for a solution of semi-flexible polymers at large frequencies, which has been verified recently by two research groups (Gittes et al., 1997; Palmer et al., 1998).

The concentration dependence of the mean-square displacement allows to gain insight into the nature of the interactions between the probing bead and the polymer network at short times. If we rescale the short-time displacement at different actin concentrations by $(c/24 \mu\text{M})^{1/2}$, choosing the 24 μM solution as standard, the mean-square displacements at other concentrations overlap for the entire concentration range, i.e. both for the isotropic phase and the anisotropic phase (see Fig. 2). Therefore, at short time scales, the mean square displacement scales as

$$\langle \Delta r^2(t) \rangle \propto c^{-1/2} \quad t \ll \tau_e \quad (14)$$

with actin concentration. This result is unexpected since one would anticipate the viscoelastic modulus to be linearly dependent on concentration at large frequencies, or equivalently $\langle \Delta r^2(t) \rangle \propto c^{-1}$.

A possible explanation for this scaling law, given by Maggs (1997), is that the displacement of the microspheres at short time scales is dominated by hydrodynamic interactions. The total dissipation of the bead is order $\approx \eta(v^2/\xi^2)(a^2\xi_h)$ since the hydrodynamic flow created by the moving bead is screened into the solution, and is non-negligible up to a distance ξ_h into the sample from the bead. Here, η is the solvent viscosity, v is the velocity of the bead, and ξ_h is of the order of the

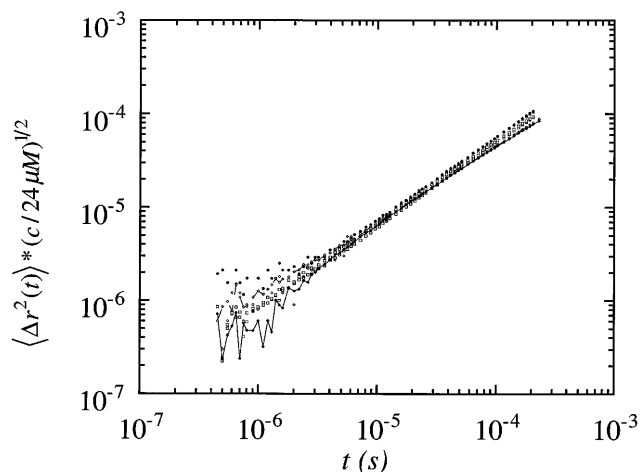


Fig. 2 Overlap of the small-time scale mean-square displacement measurements rescaled by $(c/24 \mu M)^{1/2}$

mesh size ξ . Since $\xi_h \approx \xi \propto c^{-1/2}$ for a solution of semi-flexible polymers for which $l_p \gg (\xi, l_e)$ and $\langle \Delta r^2(t) \rangle$ is approximately inversely proportional to the friction, then the friction is proportional to $c^{1/2}$, in qualitative agreement with our observations. However, this reasoning is approximate here since the motion of the bead is not diffusive even at the shortest time scales probed by DWS; therefore one cannot associate a *constant* friction coefficient to the bead.

As shown in Fig. 1, at intermediate time scales and over a wide temporal range, the exponent α decreases progressively to values much smaller than $3/4$. This corresponds to the progressive elastic trapping of the bead by the cage formed by the surrounding actin polymers. As verified by video-microscopy, electron microscopy, and analytical centrifugation (not shown here), the trapping or caging of the bead by the network is entropic in origin because the bead does not bind to actin.

Diffusion coefficient and velocity autocorrelation function

Mean square displacements can be further analyzed in terms of a time-dependent diffusion coefficient. Figure 3a shows the diffusion coefficient defined as

$$D(t) \equiv \langle \Delta r^2(t) \rangle / 6t \quad (15)$$

and calculated from the data in Fig. 1. We observe that the motion of a microsphere cannot be described by a single diffusion coefficient, but by a diffusion coefficient which varies with time. At short times and corresponding small length scales, the microspheres experience the small amplitude, high-frequency lateral fluctuations of the subsections of the actin filaments between entanglements. At long times and long length scales,

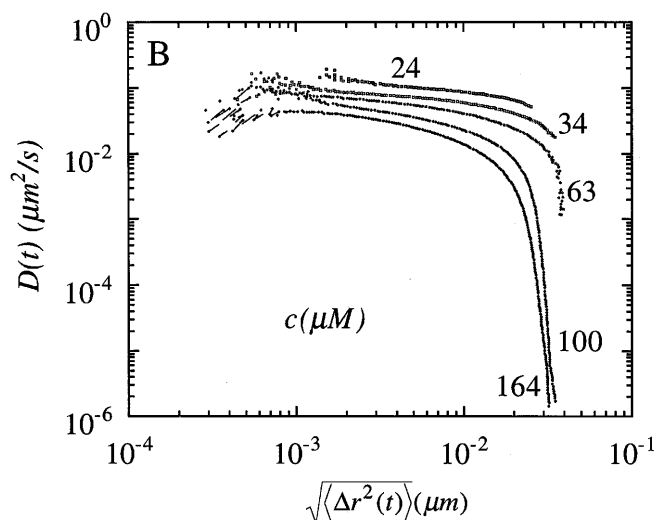
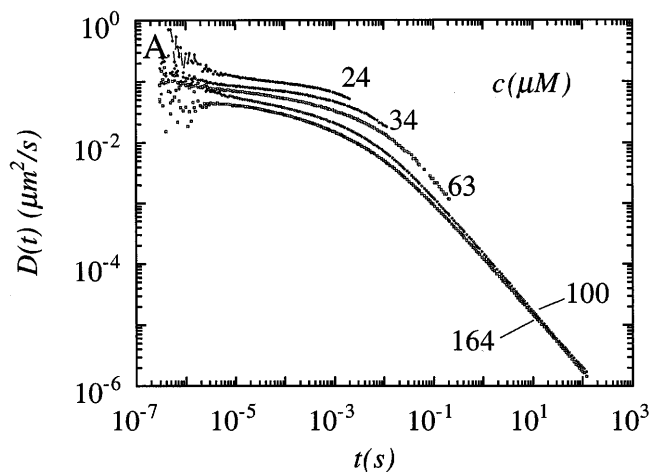


Fig. 3 **A** Time-dependent diffusion coefficient of a microsphere embedded in an actin solution. The diffusion coefficient is defined by $D(t) \equiv \langle \Delta r^2(t) \rangle / 6t$ and calculated from the data in Fig. 1. **B** Diffusion coefficient D as a function of the average displacement of the microsphere $\sqrt{\langle \Delta r^2 \rangle}$

the microsphere becomes elastically trapped by the actin mesh.

The associated diffusion coefficient D of the probing microsphere is non-constant and spans almost five decades. The diffusion coefficient varies from $D \approx 10^{-6} \mu m^2/s$ for large actin concentrations and long times to $D \approx 0.3 \mu m^2/s$ for small actin concentrations and short times (see Fig. 3A). The former value corresponds to near-arrest of the microsphere by the elastic actin network: the microsphere probes the elasticity of the actin mesh at long times. The latter is close to but smaller than the diffusion coefficient of the same microsphere in water of viscosity 1 cP, which is equal to $D_0 = k_B T / 6\pi\eta a \approx 0.46 \mu m^2/s$. If the bead size were

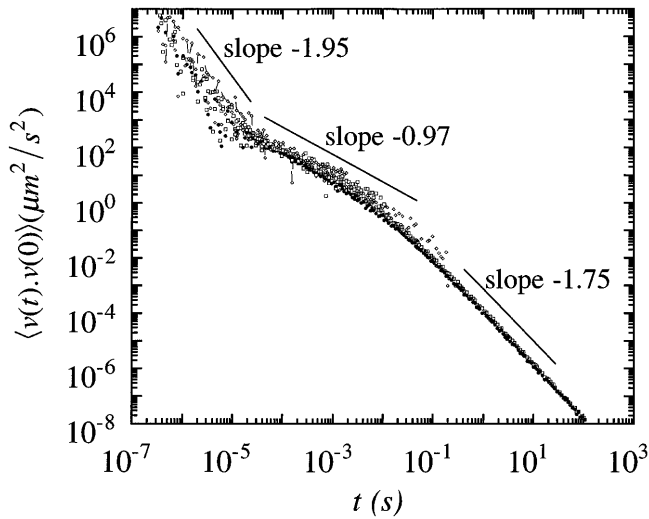


Fig. 4 Velocity autocorrelation function $\langle v(t)v(0) \rangle$ of a microsphere in an actin solution

much smaller than the mesh size, actin would not hinder its diffusion and D would be D_0 . When the bead size is much larger than the mesh size (which is the case in the present work), actin rapidly hinders the bead's motion as shown in Fig. 3 A.

To establish the relation between the diffusion coefficient and the local displacement of microsphere, we plot D as a function of $\sqrt{\langle \Delta r^2 \rangle}$ (see Fig. 3 B). This figure shows two distinct dynamical regions. First, a slow near-plateau at short length scales, then a sharp downward transition past a characteristic crossover length scale. This crossover length scale decreases from ≈ 20 to 2 nm when actin concentration is increased from 24 to 164 μM . Over the same concentration range, this crossover length scale is always much smaller than the average mesh size of the actin network, which varies from ≈ 150 to 60 nm over the concentration range investigated here.

The values of D that we measured by DWS can be compared with values obtained using classical dynamic light scattering by Newman et al. (Newman et al., 1989). These authors measured the diffusion coefficient of latex spheres imbedded in actin solutions and obtained values ranging $D/D_0 \approx 1 - 0.2$ for 270 nm radius spheres in actin solutions of concentrations ranging $c = 1-22 \mu\text{M}$. The magnitude of these values agree with our optical measurements at least if we use D optically measured at very short times and small actin concentrations. But, as shown in Fig. 3, the diffusion of latex spheres in concentrated F-actin solutions is not well described by a single diffusion coefficient since their transport becomes subdiffusive at times as short as 10^{-4} s. Indeed, we obtain values that are 10^5 to 10^6 smaller than D_0 at long times and large actin concentra-

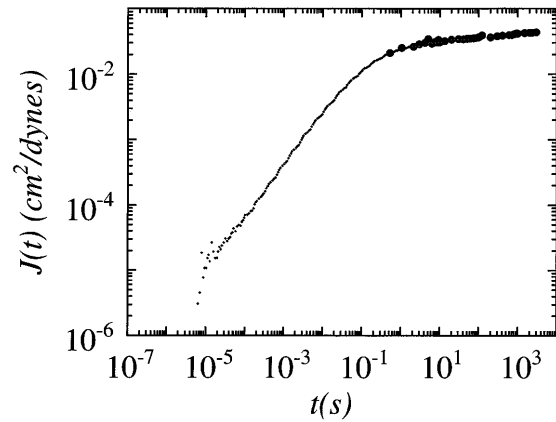


Fig. 5 Evolution of the creep compliance for a 100 μM F-actin solution as measured using DWS (closed circles), single particle-tracking microrheology (closed squares) and mechanical rheometry (open symbols)

tions. Moreover, the interpretation of dynamic light scattering data at high actin concentrations becomes difficult (if not incorrect) because of the multiply-scattered nature of the light intensity.

The displacement of a microsphere in a solution of semi-flexible polymers can be further studied by calculating the velocity autocorrelation function $\langle v(t)v(0) \rangle$, as shown in Fig. 4. The function $\langle v(t)v(0) \rangle$ is defined as

$$\langle v(t)v(0) \rangle = -\frac{dD(t)}{dt} \quad (16)$$

Figure 4 shows the extreme sensitivity of DWS, since $\langle v(t)v(0) \rangle$ varies more than 14 decades over the probed temporal range. The autocorrelation function $\langle v(t)v(0) \rangle$ decays via three distinct temporal regions. At short times, the velocity autocorrelation function decays as a power law of time over two decades:

$$\langle v(t)v(0) \rangle \propto t^{-1.75 \pm 0.10} \quad t \ll \tau_e. \quad (17)$$

The "long-time tail" is different from that observed in dilute colloidal suspensions for which $\langle v(t)v(0) \rangle \propto t^{-3/2}$ at short times (Weitz and Pine, 1993). At intermediate times, we also observe a power law behavior with a somewhat smaller exponent, $\langle v(t)v(0) \rangle \propto t^{-0.97 \pm 0.15}$, over more than three decades. At long times, the autocorrelation functions decay again rapidly with an effective power law $\langle v(t)v(0) \rangle \propto t^{-1.75 \pm 0.10}$, also over more than three decades. We can qualitatively associate $\langle v(t)v(0) \rangle$ to the dissipation of the microsphere by interaction with the mesh, or *vice versa* the dissipation due to the lateral fluctuations of subsections of the polymers between entanglements. Dissipation is proportional to v^2 which scales as $t^{-1.75}$, suggesting that the dissipation or loss modulus is large at short time scales, scaling as

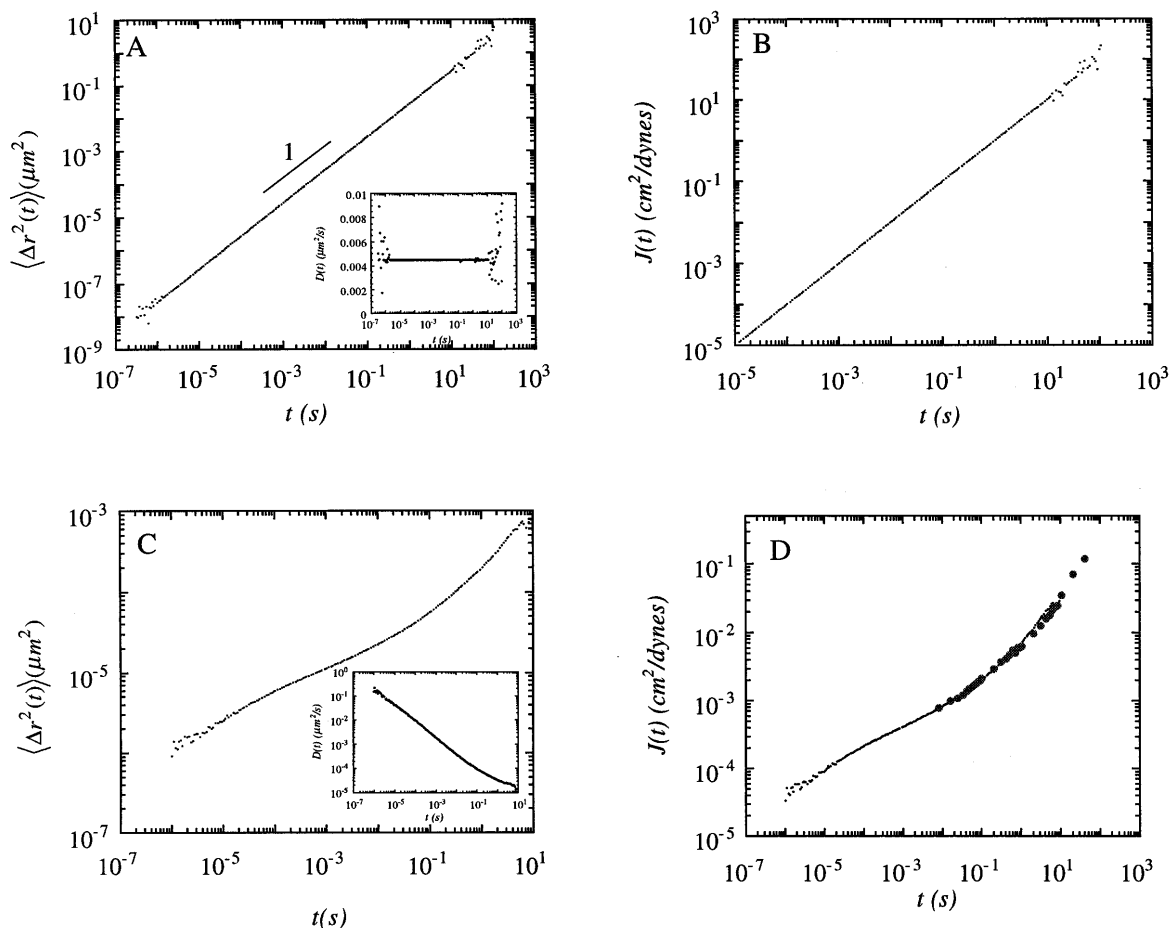


Fig. 6 Evolution of the mean square displacement and of the creep compliance of solutions of flexible polymers and a purely viscous fluid. **A** Mean square displacement and diffusion coefficient of 0.96 μm diameter microspheres in a 1 P viscous oil. **B** Creep compliance measured by DWS (closed circles) and mechanical rheometry (open circles) of a 1 P viscous oil. The inverse of the slope yields a viscosity of 1.03 P. **C** Mean square displacements and corresponding time-dependent diffusion coefficients in three PEO/water solutions in the semi-dilute regime measured by DWS. The mean square displacement follows a power law increase with time, $\langle \Delta r^2(t) \rangle \propto t^{0.67}$ PEO-water solutions. **D** Creep compliance of PEO solutions

$G'' \propto \omega^{0.75}$ with frequency, which confirms the results of Palmer et al. (1998).

Creep compliance calculated from MSD measurements and measured by mechanical rheometry

We now directly test Eq. (9), which relates the mean square displacement $\langle \Delta r^2(t) \rangle$ of a microsphere in a fluid to the shear compliance $J(t)$ of that fluid. We calculate $J(t)$ from our high-resolution mean square displacement measurements and compare these calculated values to $J(t)$ measured by a stress-controlled rheo-

meter. Figures 5–7 demonstrate the remarkable agreement between our optical and mechanical measurements of $J(t)$ for systems as diverse as a viscous oil, solutions of flexible polymers, and solutions of semi-flexible polymers. Because of the limited overlap of the two optical and mechanical approaches, this agreement can be tested at intermediate time scales only.

This agreement supports our new interpretation of the mean-square displacement, supports the use of particle-tracking rheometry to probe the local compliance of a polymer system or complex fluids, and eliminates the extra transformations for the calculation of the viscoelastic moduli. Indeed, our creep compliance measurements, being proportional to the “raw” data generated by DWS and particle-tracking, do not crop small and large frequencies out of calculated values of the viscoelastic moduli. Figures 5–7 also show the complementarity of particle-tracking measurements and classical mechanical measurements. Very short time scales are inaccessible to classical mechanical rheometry. *Vice versa*, very long time scales are inaccessible to optical rheometry and particle-tracking rheometry.

Figure 5 displays the creep compliance of a 100 μM actin solution. Creep compliance is measured using

both particle-tracking micro-rheology and classical mechanical rheometry. We observe excellent agreement over the temporal range probed by mechanical rheometry. Of course, since mean-square displacement and creep compliance are proportional, the shape of the $J(t)$ curve is identical. Therefore, the discussion given above regarding the short- and long-time behavior of $\langle \Delta r^2(t) \rangle$ holds for $J(t)$, including the concentration dependence of $J(t)$ at short time scales.

The present work is primarily concerned with solutions of semi-flexible polymers, but in order to further test Eq. (9), we conduct two “control” experiments. The first one involves a purely viscous fluid, a viscous of fixed viscosity $\eta=1.03$ P. Figure 6 displays the mean-square displacements measured by DWS, the diffusion coefficient, and the corresponding creep compliance. We first verify that the motion of the microsphere is purely diffusive since the log-log plot in Fig. 6A yields a linear increase of the mean square displacement with a slope of $\alpha=1.03\pm 0.02$. We expect this result since the motion of a Brownian sphere in a viscous fluid should be purely diffusive and $\langle \Delta r^2(t) \rangle = (k_B T / \pi a \eta) t H(t)$ at long times. The diffusion coefficient of a $0.96 \mu\text{m}$ diameter microsphere in a 1.03 P viscous oil is predicted to be $D_0 = k_B T / 6\pi \eta a = 4.4 \times 10^{-3} \mu\text{m}^2/\text{s}$, which we measure using DWS as shown in Fig. 6A. Finally, according to Eq. (9), we expect $J(t) = (t/\eta)H(t)$, which we obtain as shown in Fig. 6B. The slope in Fig. 6b yields a bulk viscosity $\eta=1.03\pm 0.05$ P, which is the correct viscosity of the oil. This result shows that particle-tracking measurements are not limited to viscoelastic fluids such as F-actin solutions, but can probe purely viscous fluids. This agreement also confirms that our new approach is quantitative.

The second control experiment involves the measurement of the creep compliance of a viscoelastic solution of flexible polymer, an aqueous solution of polyethylene oxide. Here again, we conduct DWS measurements and classical creep compliance measurements. Figure 6c displays the mean square displacement and the diffusion coefficient; Fig. 6d displays calculated and measured creep compliance. The same level of agreement as for the actin solutions and the viscous oil is found for the semi-dilute solution of flexible polymer.

The agreement of DWS and video-enhanced SPT measurements with mechanical measurements at long times can be considered surprising. As pointed out by Gittes et al. (1997), the viscous solvent moves together with the probed network at frequencies larger than $\omega_c \approx G \xi^2 / \eta a^2$, where G is the modulus of the actin network, ξ is the mesh size, and η is the viscosity of the buffer. This last expression is obtained by the balance between viscous and elastic force actin on the microsphere. The formalism presented in the Theory section describes the Brownian dynamics of a micro-

sphere at times $t < t_c = \omega_c^{-1}$. We estimate this characteristic time to be order $t_c \approx 1-0.03$ s. Therefore, the observed agreement between our mechanical measurements, which are limited to times longer than 0.007 s, and our optical measurements at times $t > t_c$ is somewhat unexpected.

Concentration dependence of the compliance

Figure 7 displays the time-dependent compliance of actin solutions for concentrations between 10 and $164 \mu\text{M}$ as measured by DWS. Since the shear compliance is proportional to the mean square displacement, the description and discussion of these measurements are identical to that offered above for the mean-square displacements. Figures 8 and 9 display the value of $J(t)$ as a function of actin concentration, at different sampling times. At short times, we find that $J(t)$ is weakly dependent on actin concentration,

$$J \propto c^{-0.53} \quad t \ll \tau_e \quad (18)$$

for $t=10^{-5}$ s and for $c < 60 \mu\text{M}$. However, at long times, this concentration dependence becomes steeper,

$$J^{(0)} \propto c^{-1.3 \pm 0.2} \quad t \gg \tau_e \quad (19)$$

for $t=10^2$ s and for $c < 60 \mu\text{M}$. At these long time scales the creep and, correspondingly, the mean-square displacement is not strongly dependent on time. On the same figure, we show video-enhanced particle-tracking microrheological measurements of the plateau compliance. Figure 9 shows the excellent agreement between DWS and single-particle-tracking measurements. The

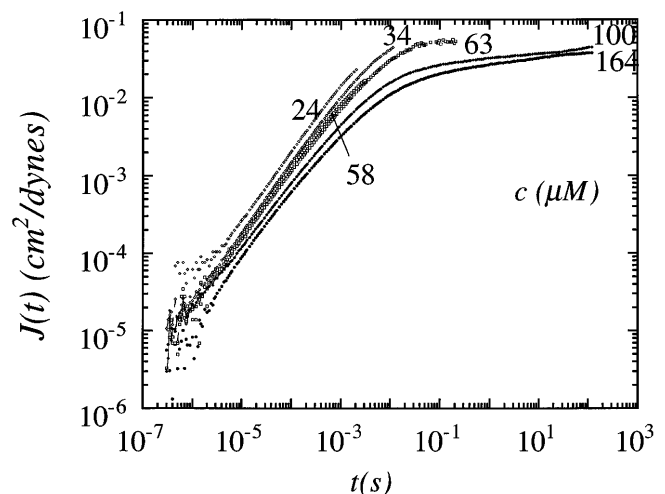


Fig. 7 Evolution of the shear creep compliance for F-actin solutions with concentrations ranging from 10 to $164 \mu\text{M}$. A creep compliance “plateau” is reached faster and at a lower value for increasing actin concentration, reflecting both the decreasing size of the actin mesh and the corresponding increase of the elasticity of the network

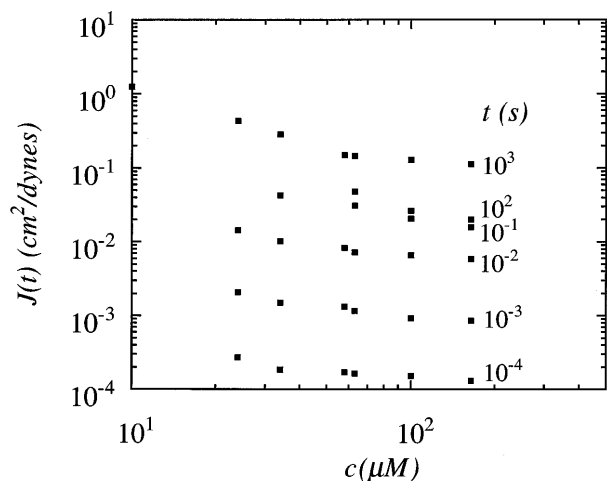


Fig. 8 Values of $J(t)$ as a function of actin concentration at different sampling times. Note the saturation of the creep compliance for actin concentrations larger than $\approx 50 \mu\text{M}$, which corresponds to the onset of a liquid crystalline ordering in the system

concentration dependence of the plateau compliance for actin is much weaker than predicted for semi-dilute solutions of flexible polymers, for which $J^{(0)} \propto c^{-2.2}$ (Doi and Edwards, 1989).

Using Morse's model of shear rheology of actin solutions, we can attempt to explain the unusual concentration dependence of the creep compliance. According to Morse's model, the long-time shear modulus of a solution of semi-flexible polymers can be described by the classical expression $G(t) = G^{(0)} \sum_{p, \text{odd}} (8/p^2 \pi^2) \exp(-p^2 t / \tau_D)$ of the de Gennes-Doi-Edwards model of reptation (Doi and Edwards, 1989). Here, $G^{(0)}$ is the plateau modulus and τ_D is the terminal relaxation time of the polymer, i.e. the time necessary for an actin filament to disengage from its initial tube. Therefore, the steady state compliance is predicted to be $J^{(0)} = \int_0^\infty t G(t) dt / [\int_0^\infty G(t) dt]^2 = 6/5 G^{(0)}$ (Doi and Edwards, 1989).

For actin solutions, $G_p' > G_p''$ at long times, hence $G^{(0)} \approx G_p'$ and the compliance is of the order of the inverse of the small-frequency elastic modulus, $J^{(0)} \propto 1/G_p'$. Morse predicts that the concentration dependence of the elastic plateau modulus depends on concentration as $G_p' \propto c^{7/5}$, which has recently been verified experimentally by both optical and mechanical rheometry (Xu et al., 1998b). Therefore, $J^{(0)} \propto c^{-7/5}$, in agreement with our mechanical, DWS, and particle-tracking measurements (see Fig. 9). Therefore, the origin of the long-time creep is due to the reptation of the long semi-flexible polymers (Morse, 1997). However, this argument is approximate and would be correct if $J(t)$ were a true plateau and if a F-actin network were an elastic solid. Our recent work shows that, at equilibrium, actin rheology is indeed solid-like, but with a

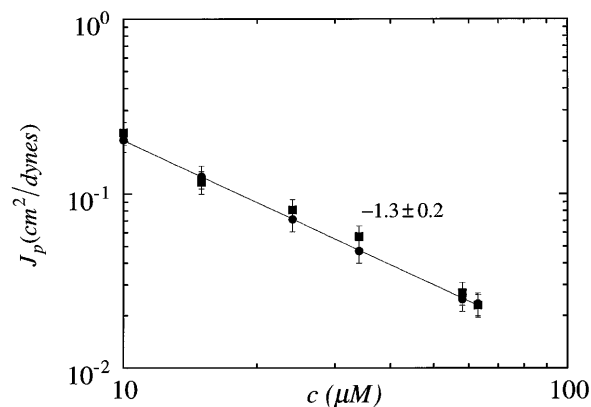


Fig. 9 Plateau shear compliance for F-actin solutions as a function of actin concentration c . The magnitude of the plateau is arbitrarily defined as J_p . The shear compliance plateau evaluated at 10^3 s increases with actin concentration as $J_p \propto c^{-1.3 \pm 0.2}$. This figure shows the excellent agreement between DWS measurements (circles) and video-enhanced particle-tracking measurements (squares) of the concentration-dependent creep

non-negligible dissipative component, $G'' \approx (0.3-0.4) \times G'$ at small frequencies (Xu et al., 1998b). A more formal expression, which specifically predicts the (time-dependent) shear creep compliance of a solution of semi-flexible polymers is therefore needed to compare our new data to a model.

Summary and conclusions

This paper predicts the proportionality between the mean square displacement of a microsphere imbedded in a fluid and the local linear creep compliance of that fluid. We test this relation using mechanical rheometry, diffusing wave spectroscopy, and particle-tracking microrheometry on three different systems: a purely viscous oil, a viscoelastic solution of flexible polymers, and a viscoelastic solution of semi-flexible polymers. Mechanical rheometry measures the creep directly by applying a small stress and by measuring the resulting strain. This conventional measurement is macroscopic. Instead, our particle-tracking microrheology instruments measure the mean-square displacement resulting from the thermal energy imparted to a small microsphere suspended in the same system. This measurement is mesoscopic because it is conducted at length scales much smaller than the sample size and the actin filaments, but still much larger than the mesh size and the small solvent molecules. We observe excellent agreement for three different systems over the temporal range shared by the mechanical and optical instruments.

These instruments are complementary: while mechanical rheometry is best suited to probe the long-time

creep behavior of polymer solutions, DWS is best suited to probe short time scales, from 10^{-6} to 10^2 s. Video-based SPT is not as accurate as DWS, but uses much smaller amounts of sample and is straightforward to implement.

In the case of a solution of semi-flexible polymers, we observe that the creep compliance scales as $J(t) \propto t^{0.78 \pm 0.05}$ at short times, which is a direct consequence of the rigidity of actin. At long times, the shear compliance reaches a quasi-plateau, which decreases with concentration as $J \propto c^{-1.2 \pm 0.3}$. This concentration

dependence is also a direct consequence of the finite rigidity of actin. We are currently testing Eq. (9) on other polymer systems such as solutions of microtubules, which are rigid polymers, and colloidal systems, such as clays.

Acknowledgments The authors acknowledge D. Morse and A.C. Maggs for helpful discussions, and thank A. Palmer, K. Rufener and T.G. Mason for their help in the DWS measurements. D.W. acknowledges financial support from the Whitaker Foundation and the National Science Foundation, grants DMR 9623972 (CAREER), CTS 9502810, and CTS 9625468.

References

- Alberts B, Bray D, Lewis J, Rabb M, Roberts K, Watson J (1994) *Molecular Biology of the Cell*, Garland Publishing, New York
- de Gennes P-G (1979) *Scaling Concepts in Polymer Physics*, Cornell University Press, New York
- Doi M, Edwards SF (1989) *The Theory of Polymer Dynamics*. Clarendon Press, Oxford
- Ferry JD (1980) *Viscoelastic Properties of Polymers*. John Wiley and Sons, New York
- Gittes F, Mickey B, Nettleton J, Howard J (1993) Flexural rigidity of microtubules and actin filaments measured from thermal fluctuations in shape. *J Cell Biol* 120:923–934
- Gittes F, Schnurr B, Olmsted PD, Macintosh FC, Schmidt CF (1997) Microscopic viscoelasticity: shear moduli of soft materials determined from thermal fluctuations. *Phys Rev Lett* 79:3286–3289
- Haskell J, Newman J, Selden LA, Gershman LL, Estes JE (1994) Viscoelastic parameters for gelsolin length regulated actin filaments. *Biophys J* 66:A196
- Isambert H, Venier P, Maggs AC, Fattoum A, Kassab R, Pantaloni D, Carlier M-F (1995) Flexibility of actin filaments derived from thermal fluctuations. *J Biol Chem*. 270:11437–11444
- Janmey PA, Hvidt S, Käs J, Lerche D, Maggs A, Sackmann E, Schliwa M, Stossel TP (1994) The mechanical properties of actin gels. *J Biol Chem* 269:32503–32513
- Janmey PA, Hvidt S, Lamb J, Stossel TP (1990) Resemblance of actin-binding protein/actin gels to covalently networks. *Nature* 345:89–92
- Janmey PA, Hvidt S, Peetermans J, Lamb J, Ferry JD, Stossel TP (1988) Viscoelasticity of F-actin/gelsolin complexes. *Biochemistry* 88:8218–8227
- MacLean-Fletcher SD, Pollard TD (1980) Viscometric analysis of the gelation of acanthamoeba extracts and purification of two gelation factors. *J Cell Biol* 85:414–428
- Maggs AC (1997) Personal communication
- Mason TG, Dhople A, Wirtz D (1997a) In: Wirtz D, Halsey TC (eds) *Statistical Mechanics in Physics and Biology*, pp 153–158
- Mason TG, Ganesan K, van Zanten JV, Wirtz D, Kuo SC (1997b) Particle-tracking microrheology of complex fluids. *Phys Rev Lett* 79:3282–3285
- Mason TG, Weitz D (1995) Optical measurements of frequency-dependent linear viscoelastic moduli of complex fluids. *Phys Rev Lett* 74:1254–1256
- Morse D (1997) *Macromolecules preprint*
- Muller O, Gaub H, Barmann M, Sackmann E (1991) Viscoelastic properties of sterically and chemically cross-linked actin networks in the dilute and semidilute regime: measurements by an oscillating disk rheometer. *Macromolecules* 24: 3111–3120
- Newman J, Schick KL, Zaner KS (1989) Probe diffusion in cross-linked actin gels. *Biopolymers* 28:1969–1980
- Palmer A, Xu J, Wirtz D (1998) High-frequency rheology of crosslinked actin networks measured by diffusing wave spectroscopy. *Rheologica Acta* 37:97–106
- Sato M, Schwarz WH, Pollard TD (1987) Dependence of the mechanical properties of actin/ α -actinin gels on deformation rate. *Nature* 325:828–830
- Schnurr B, Gittes F, MacKintosh FC, Schmidt CF (1997) Determining microscopic viscoelasticity in flexible and semiflexible polymer networks from thermal fluctuations. *Macromolecules* 30: 7781–7790
- Spudich JA, Watt S (1971) The regulation of rabbit skeletal muscle contraction. *J Biol Chem* 246:4866–4871
- Tempel M, Isenberg GES (1996) Temperature-induced sol-gel transition and microgel formation in α -actinin cross-linked actin networks: a rheological study. *Phys Rev E* 54:1802–1808
- Wachsstock D, Schwarz WH, Pollard TD (1993) Affinity of α -actinin for actin determines the structure and mechanical properties of actin filament gels. *Biophys J* 65:205–214
- Wachsstock D, Schwarz WH, Pollard TD (1994) Crosslinker dynamics determine the mechanical properties of actin gels. *Biophys J* 66:801–809
- Weitz DA, Pine PJ (1993) In: Wyn B (ed) *Dynamic Light Scattering*. Oxford University Press, Oxford
- Xu J, Schwarz WH, Käs JA, Stossel TP, Janmey PA, Pollard TD (1998a) Mechanical properties of actin filament networks depend on preparation, polymerization conditions, and storage of actin monomers. *Biophys J* 74:2731–2740
- Xu J, Palmer A, Wirtz D (1998b) Viscoelastic of solutions of semiflexible polymers measured by mechanical rheology and particle-tracking microrheology: actin filament networks. *Macromolecules*, accepted for publication
- Xu J, Wirtz D, Pollard TD (1998c) Dynamic cross-linking by α -actinin determines the mechanical properties of actin filament networks. *J Biol Chem* 273:9570–9576
- Zaner KS, Hartwig JH (1988) The effect of filament shortening on the mechanical properties of gel-filtrated actin. *J Biol Chem* 263:4532–4536